Superconductor sandwiches: cuprate-manganite multilayers with a remarkable new ground state.

B.P.P. Mallett[a], P. Marsik[b], J. Khmaladze[b], R. Arul[a,d], M. Minola[c], M.C. Simpson[a,d], and C. Bernhard[b]

[a]The Photon Factory, The University of Auckland, 38 Princes St, Auckland, New Zealand
[b]University of Fribourg, Department of Physics and Fribourg Center for Nanomaterials, Chemin du Muse 3, CH-1700 Fribourg, Switzerland
[c]Max-Planck-Institut für Festkörperforschung, Heisenbergstr. 1, 70569 Stuttgart, Germany
[d]The Dodd Walls Centre for Quantum and Photonic Technologies, 38 Princes St, New Zealand

ABSTRACT

A remarkable new electronic ground-state of a high-temperature superconductor oxide ($YBa_2Cu_3O_{7-\delta}$) is found when it is grown in-between layers of a specific manganite ($Pr_{0.5}La_{0.2}Ca_{0.3}MnO_3$). The superconductor in these 'superconductor sandwiches' apparently adopts an exotic granular-state due to an interaction with the manganite. Uniquely, a strong magnetic field recovers a more 'customary' superconducting state. Here we show how Raman spectroscopy, state-of-the-art THz ellipsometry, and transport measurements are being used to reveal the nature of this new ground-state. These measurements are shedding light on how the manganite and superconductor layers interact to cause such novel behaviour, however the exact mechanism remains unknown.

Keywords: superconductor, manganite, multilayer, magnetism, thin film, interface, emergent properties

1. INTRODUCTION

The quantum phase transition from a superconducting (SC) to a metallic, or even insulating, state is of great scientific and technological interest.[1,2] Normally it is induced by structural disorder, electronic doping, or decreasing the layer thickness of thin films. Magnetic fields can also induce such a quantum phase transition as they almost always reduce SC phase coherence. In the wide literature of superconductivity, there are however only three examples known where a magnetic field *restores* SC phase coherence. In the bulk, these include the chevrel phase $Eu_xSn_{1+x}Mo_6S_8$[3] and the organic λ-$(BETS)_2FeCl_4$[4,5] whereby the magnetic field compensates an internal field from magnetic ions (Jacarino-Peter effect),[6] or suppresses detrimental magnetic fluctuations.[7] In reduced dimensional systems, a reentrance of SC was reported in Zn nanowires where the field seems to reduce quantum fluctuations by generating dissipative quasi-particles.[8,9]

Recently, we showed that another, distinct kind of these rare cases can be found in cuprate/manganite multilayers.[10] In these 'superconductor sandwiches', an interaction ~ 5 nm either side of the interface between a $YBa_2Cu_3O_{7-\delta}$ (YBCO) layer and a $Pr_{0.5}La_{0.2}Ca_{0.3}MnO_3$ (PLCMO) layer induces a novel ground state in the YBCO with a high-resistance. Surprisingly, a magnetic field restores a coherent SC state with in the YBCO. This magnetic-field-driven recovery of SC phase coherence is likely due to the field suppressing an interaction between the YBCO and PLCMO that is detrimental to macroscopic SC coherence, despite it also significantly enhancing ferromagnetic order in the PLCMO.[10,11] The interaction is clearly sensitive to the precise nature of the PLCMO properties since such effects have not been seen in the comparatively well studied YBCO-$La_{0.7}Ca_{0.3}MnO_3$ multilayers,[12–15] where there has not been a partial substitution of Pr^{3+} for La^{3+} in the manganite.

Here we summarize the phenomenology of the YBCO/PLCMO multilayers to date and present recent Raman spectroscopy results. Such ongoing investigations are starting to reveal nature of this novel ground state and interactions in YBCO/PLCMO multilayers which, aside from being fundamentally and technologically interesting in its own right, offers a new window on the physics of these two fascinating strongly-correlated material systems.[16–18]

Send correspondence to BPPM, e-mail: b.mallett@auckland.ac.nz

2. RESULTS

2.1 Samples and methods

PLCMO/YBCO thin film multilayers were grown on on $La_{0.3}Sr_{0.7}Al_{0.65}Ta_{0.35}O_3$ (LSAT) substrates by pulsed laser deposition, details are given in Refs.[10,19] Typically trilayers are grown with film thicknesses 20-7-20 nm, however similar interaction effects are seen in PLCMO-YBCO bilayers and superlattices. A combination techniques - e.g. x-ray reflection and diffraction (XRR, XRD), transmission electron microscopy (TEM) and electron energy-loss spectroscopy (EELS) - show that the multilayers are epitaxial with high structural and chemical quality and chemically sharp interfaces between the PLCMO and YBCO.

Magneto-resistance and vibrating sample magnetometry (VSM) measurements were made in a Quantum Design PPMS, and used specialised electronics for the transport measurements. The optical response was determined with spectroscopic ellipsometry. In the terahertz (THz) region (3-70 cm^{-1}) we used a home-built time-domain THz ellipsometer,[20,21] in the infrared (70-4000 cm^{-1}) a home-build setup attached to a Bruker 113v Fourier-transform spectrometer (FTIR)[22] and, a Woollam VASE ellipsometer in the near-infrared to ultraviolet (4000-52000 cm^{-1}).Raman spectroscopy measurements were made using LabRam spectrometer in back-scattering geometry with a 633 nm laser line. A z-scan method was used to remove the substrate contribution to the signal.[23]

2.2 Electrical transport

Figure 1a shows the resistance vs temperature (R-T) in a few select magnetic fields for a PLCMO/YBCO/PLCMO trilayer sample of film thickness 20-7-20 nm. All data are were obtained whilst cooling with the magnetic field set at 300 K (i.e. field-cooled) and were measured with a 4-wire resistance configuration with a constant 10 μA excitation current.

Above 80 K the data reveal nothing unusual and reflect the metallic-like response the normal state of YBCO, with possible additional conduction through the PLCMO layer above 225 K. At low temperatures however, in low fields the R-T turns up sharply. In parallel, the magneto-resistance becomes very large and strongly hysteretic,[10] and there are pronounced *intrinsic* fluctuation effects which lead to large jumps in the R-T curves, as seen for example in the data taken at 4 T magnetic fields.

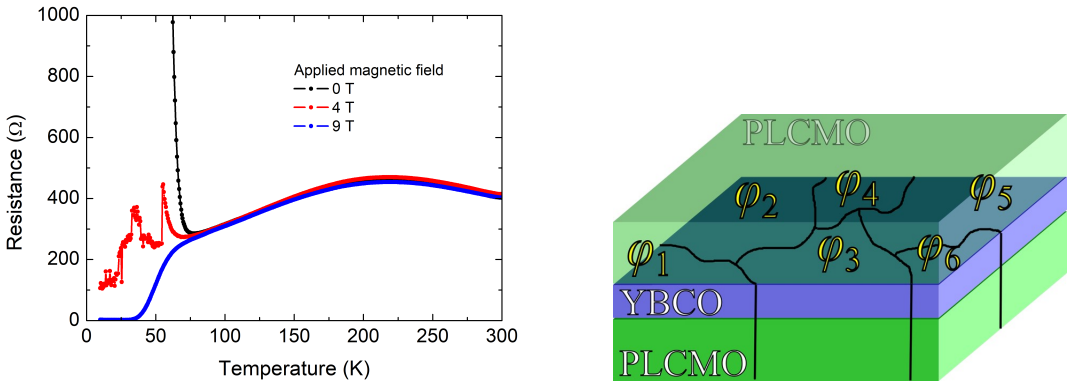

Figure 1. (a) Typical resistance vs temperature data for a PLCMO/YBCO multilayer ('superconductor sandwiches'). The large drop in resistance with magnetic field at low temperature indicates magnetic-field driven superconducting coherence. (b) An illustration of the proposed low temperature and field state of the PLCMO/YBCO multilayers. The phase, φ, of superconductor wavefunction is locally coherent, but globally incoherent (multi-valued) and pinned to order in the PLCMO.

In higher-fields, a more conventional-looking superconducting transition is recovered - an indication of the field-driven SC coherence. At 9 T, the R-T curves resembles that of a traditional superconducting transition*, with corresponding I-V characteristics that one would expect from a coherent SC state.[10]

*The small residual R may be related to the top contact geometry and trapped charges in the upper PLCMO layer, or may signal a field larger than 9 T is required to fully restore phase coherence.

This phenomenology is distinct from the basic resistivity behaviour of the materials by themselves; YBCO films show a SC transition at about 80 K (the value depends on factors such as the oxygen doping) that broadens and shifts to lower temperatures in magnetic fields. The PLCMO undergoes a magnetic-field induced insulator-to-metal transition,[11] but this transition is over a broad temperature range (rather than the sharp effect at 80 K in the multilayers) and the transition is incomplete at 9 T for our material, i.e. PLCMO remains insulating across the entire temperature range and field range studied here.

2.3 THz to optical spectroscopy

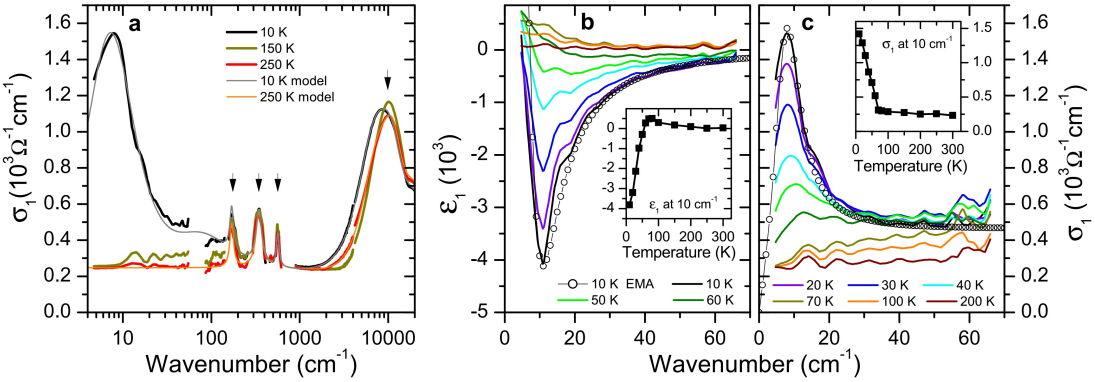

Figure 2. The optical response of the PLCMO/YBCO multilayers obtained by ellipsometry, from Ref.[10]

The *R-T* curves in figure 1 show similarities with the ones of a granular SC.[1] It is however THz and infrared spectroscopy at zero-field that provides critical additional evidence for such confinement of the Cooper-pairs on a mesoscopic scale.

Figure 2a shows the real part of the optical conductivity, σ_1, due to the combined response of the PLCMO and YBCO layers, as measured by spectroscopic ellipsometry.[10] The main features at 250 K are a strong peak around $10,000$ cm^{-1} due to the lowest *d-d* interband transition of PLCMO, three narrow modes at 175, 345, and 565 cm^{-1} due to infrared-active phonon modes, and a finite conductivity at low-frequency that is assigned to the metallic response of the trilayer.

Notably, at low temperatures the low-frequency response undergoes significant changes, as highlighted in figures 2b and c. The downturn of ϵ_1 to large negative values signals a strong enhancement of the inductive response that is typical for a loss-free SC condensate. In contrast to a bulk SC state however, the spectral weight of the condensate in σ_1 is contained in a narrow mode at about 7 cm^{-1} instead of a delta function at the origin. The open symbols in Figs. 2b and c show that the THz data can be described with a phenomenological effective medium model of SC grains that are separated by a dielectric layer, but which have a SC condensate density typical for YBCO in just such a thin-film. However, as outlined in Ref.,[10] it yields an unrealistically small volume fraction of the dielectric suggesting that a more sophisticated model is required, for example one that explicitly takes into account interference and pair-breaking of the SC order parameter at grain boundaries.

The combined results from (on-going) optical spectroscopy and in-depth magneto-transport measurements[10] suggest the following situation. At low temperatures and fields, a phase-incoherent SC state forms due to an interaction between the YBCO and PLCMO, figure 1b. Larger magnetic fields grow the size of the phase-coherent regions so that a low-resistance state is recovered in a percolative manor.

Normally, the high-resistance state of a granular SC system is observed due to a spatial confinement of the SC state by the material's crystallite-size or film thickness.[1] Such an explanation in our case is however very unlikely since the structural and chemical characterization of our samples show they are of high-quality and do not show evidence of such granularity.[10] Furthermore, such an explanation struggles to explain how a magnetic field would restore SC coherence.

2.4 Raman spectroscopy

This puts the focus for further studies on the specific properties of PLCMO, and how they vary in magnetic field. In this endeavour, Raman spectroscopy provides valuable information and has been used previously on manganites to determine structural distortions and their relation to magnetism, charge- and orbital-ordering,[24–30] and has shown a long-range transfer of electron-phonon coupling across the interface in cuprate-manganite thin film multilayers.[31]

Figure 3 shows Raman spectra for a PLCMO/YBCO trilayer sample and a 20 nm PLCMO thin film. The trilayer sample has layer thicknesses 20-7-20 nm and a 2 nm thin $LaAlO_3$ protective capping layer. The polarisation configuration is $z(Y'X')z$ in Porto notation, where z is parallel to the crystallographic c-axes, x/y parallel to the a/b-axes[†] - i.e. the in-coming polarisation is -45 degrees to, and detected polarisation 45 degrees to, the a (or b) crystallographic axis along the Mn-O nearest-neighbour bonds. Also shown, for comparison, are comparable data from single crystals of $YBa_2Cu_3O_{6.5}$[32] and $La_{0.5}Ca_{0.5}MnO_3$.[28]

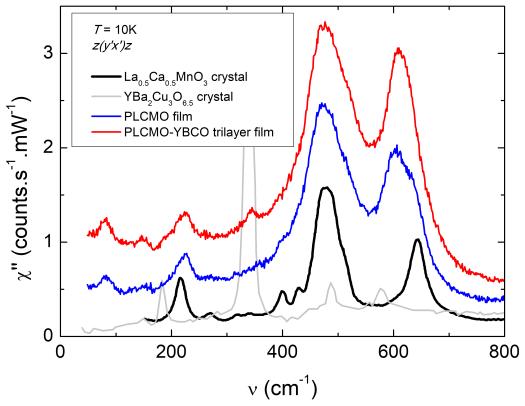

Figure 3. Representative Raman spectra for a PLCMO (20nm)/YBCO (7nm)/PLCMO (20nm) trilayer and PLCMO (20nm) layer at 10 K. Also shown, for comparison, are data from single crystals of YBCO[32] and LCMO[28] for the same $z(Y'X')z$ polarisation configuration.

Generally, the spectra show all the phonon modes expected from the single crystal data on similar materials and with comparably sharp peaks. For example, the B_{1g} mode in YBCO at 340 cm^{-1}, involving anti-phase c-axis motion of the CuO_2 layer oxygens, is clearly visible despite being only a weak feature from the 7 nm thick layer of YBCO in the trilayer sample. It has a half-width at half-maximum (HWHM) of ≈ 10 cm^{-1} (see section 4 for fitting details) which is comparable with that obtained for single crystals of YBCO[33,34] and is further indication of the good structural quality of these thin-films.

As PLCMO is the topmost layer, and as there is approximately five times as much PLCMO as YBCO in the trilayer sample, the spectral features from the former are somewhat more pronounced. We focus on a subset of these features, namely the 230 cm^{-1} and 470 cm^{-1} modes. In particular, we discuss their temperature dependence, shown in Figure 4a and b, and what they reveal about the electronic and magnetic state of the PLCMO.

Firstly we discuss the phonon mode at ≈ 230 cm^{-1}, whose temperature dependence is highlighted in figure 4b. This mode is a rotation of the MnO_6 octahedra. Its width has been seen to significantly decrease through the magnetic-ordering transition, and some report a significant hardening at the magnetic transition as well.[27,31] Both observations result from a significant spin-lattice coupling in the manganite.

In our PLCMO its position is closer to 225 cm^{-1}, and its HWHM at 10 K is about 15 cm^{-1}. Interestingly, its width decreases markedly below about 175 K concurrently with an increase in its intensity and a potential softening of its center position. This temperature is somewhat similar to the 140 K onset of a static, macroscopic magnetic moment observed by SQUID magnetometry in similar PLCMO films, and is approximately the temperature at which the electrical transport becomes non-Ohmic and hysteretic.

[†]Our samples have microscopically twinned.

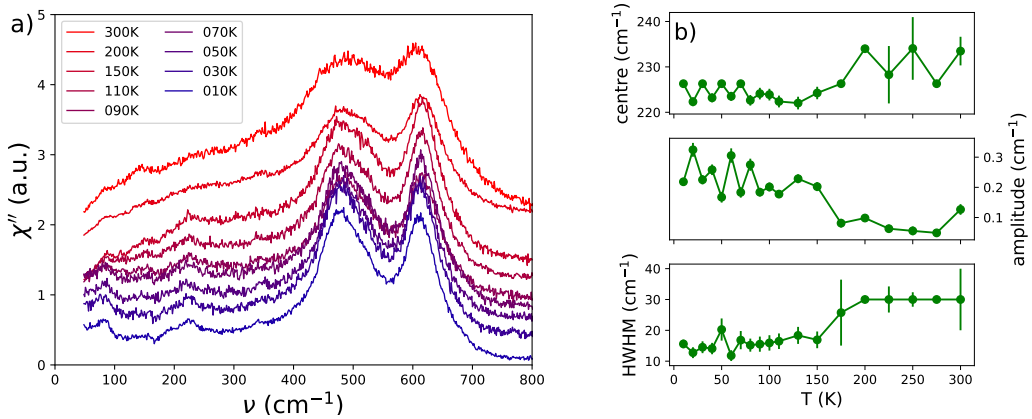

Figure 4. Temperature dependence of the Raman spectra for PLCMO/YBCO multilayer. Panel a) shows some representative bose-factor corrected data, which have been vertically shifted for clarity. Panel b) shows the temperature dependence of fit parameters describing the 230 cm^{-1} phonon mode.

The mode around 470 cm^{-1} is allowed in the presence of a (static or dynamic) Jahn-Teller distortion and involves bending the O of the MnO_6 octahedra. The intensity (peak area) and width of this mode is related to the degree of Jahn-Teller distortion and its vibration lifetime (about 10^{-12} s here) is related to the time between two consequent hops any doped charge-carrier on the Mn (e.g. the mean life time of a Mn^{3+} before a hole hops onto that site making a Mn^{4+}).[27,29] This is in turn related to the metallicity of the manganite, because the hole-hopping rate becomes faster than the Jahn-Teller mode vibration in the metallic states, resulting in a low intensity from this mode (and the 610 cm^{-1} mode).[29] On the other hand, the mode has a larger amplitude in the case of a static Jahn-Teller distortion of the Mn^{3+} octahedra - which can order with the Mn^{4+} octahedra to form the charge- and orbital-ordered insulating state. We find here that its intensity is about 8 times that of the 230 cm^{-1} A_g mode - similar to that found by others for an insulating state of the manganite.[27,28]

3. DISCUSSION AND CONCLUSIONS

Overall, the spectral features from the PLCMO are consistent with disordered $R\bar{3}c$ rhombohedral structure with phonon life time broadening of about 50 $cm^{-1} \sim 10^{-12}$ s.[29] Here, because of disorder, there is contribution from non-Γ point modes so that the phonon peaks represent the phonon-density of states.

One would expect the PLCMO structure is not going to have the exact translational symmetry of e.g. $LaMnO_3$, or $La_{0.5}Ca_{0.5}MnO_3$ as there will be some degree of random disorder on the A^{3+}/A'^{2+} sites and of the Mn^{3+}/Mn^{4+}. Additional disorder may come from oxygen non-stochiometry in the manganite. Indeed, the 470 and 610 cm^{-1} modes are about twice as broad as the lower frequency modes which suggests that the oxygen sub-lattice is more strongly distorted from the perfect perovskite structure than the A (i.e. Pr,La,Ca) and B (Mn) site sub-lattices.[29]

Overall, the Raman results appear to show that the PLCMO has charge- and orbital- ordering which is static or dynamic,[26,30] but that is less well developed/ordered than in $La_{0.5}Ca_{0.5}MnO_3$ or $YMnO_3$.[24,27] Importantly, the data also indicate the manganite remains insulating[‡] at all temperatures. Any phase transitions, relating to magnetic, charge- and orbital-ordering for example, occur around 150 K. This is a temperature that is significantly higher than the $\approx$ 80 K where we see the formation of, and magnetic-field driven reduction of, a putative granular superconducting state in PLCMO/YBCO multilayers.

[‡]Small spatially segregated regions of conducting material cannot however be ruled out since our spectra are averages over approx 100×100 μm area.

4. APPENDIX: RAMAN SPECTRA FITTING ANALYSIS

Peaks in the Raman spectra were fitted to a simple Lorentzian line-shape;

$$I_L(\nu) = \frac{A\gamma^2}{\gamma^2 + (\nu + \nu_0^2)} \tag{1}$$

Here the amplitude, A, is proportional to the area of the peak. γ is the half-width at half-maximum (HWHM).

A full spectrum is simply fitted as;

$$I(\nu) = I_{BG}(\nu) + \sum_i I_{L,i}(\nu) \tag{2}$$

with the background term simply $I_{BG}(\nu) = I_L(\nu, \nu_0 = 0) + \text{const.}$.

At least 9 peaks are needed to describe the PLCMO $z(Y'X')z$ spectra, and at least 11 peaks needed for the multilayers. Each peak is described by 3 parameters (position, amplitude and HWHM), in practice however only a subset of about 20 free parameters are used in the fit as the positions and HWHMs of many of the features are only weakly temperature dependent.

REFERENCES

[1] Gantmakher, V. F. and Dolgopolov, V. T., "Superconductor-insulator quantum phase transition," *Physics-Uspekhi* **53**(1), 1–49 (2010).

[2] Goldman, A., "Superconductor-insulator transitions," *International Journal of Modern Physics B* **24**(20n21), 4081–4101 (2010).

[3] Meul, H. W., Rossel, C., Decroux, M., Fischer, O., Remenyi, G., and Briggs, A., "Observation of magnetic-field-induced superconductivity," *Phys. Rev. Lett.* **53**, 497–500 (Jul 1984).

[4] Uji, S., Shinagawa, H., Terashima, T., Yakabe, T., Terai, Y., Tokumoto, M., Kobayashi, A., Tanaka, H., and Kobayashi, H., "Magnetic-field-induced superconductivity in a two-dimensional organic conductor," *Nature* **410**(6831), 908–910 (2001).

[5] Balicas, L., Brooks, J. S., Storr, K., Uji, S., Tokumoto, M., Tanaka, H., Kobayashi, H., Kobayashi, A., Barzykin, V., and Gor'kov, L. P., "Superconductivity in an organic insulator at very high magnetic fields," *Phys. Rev. Lett.* **87**, 067002 (Jul 2001).

[6] Jaccarino, V. and Peter, M., "Ultra-high-field superconductivity," *Phys. Rev. Lett.* **9**, 290–292 (Oct 1962).

[7] Maekawa, S. and Tachiki, M., "Superconducting phase transitions in rare-earth compounds," *Phys. Rev. B* **18**, 4688–4705 (Nov 1978).

[8] Tian, M., Kumar, N., Xu, S., Wang, J., Kurtz, J. S., and Chan, M. H. W., "Suppression of superconductivity in Zinc nanowires by bulk superconductors," *Phys. Rev. Lett.* **95**, 076802 (Aug 2005).

[9] Chen, Y., Snyder, S. D., and Goldman, A. M., "Magnetic-field-induced superconducting state in Zn nanowires driven in the normal state by an electric current," *Phys. Rev. Lett.* **103**, 127002 (Sep 2009).

[10] Mallett, B. P. P., Khmaladze, J., Marsik, P., Perret, E., Cerreta, A., Orlita, M., Biškup, N., Varela, M., and Bernhard, C., "Granular superconductivity and magnetic-field-driven recovery of macroscopic coherence in a cuprate/manganite multilayer," *Phys. Rev. B* **94**, 180503 (Nov 2016).

[11] Tokura, Y. and Tomioka, Y., "Colossal magnetoresistive manganites," *Journal of Magnetism and Magnetic Materials* **200**(1?3), 1 – 23 (1999).

[12] Peña, V., Sefrioui, Z., Arias, D., Leon, C., Santamaria, J., Martinez, J. L., te Velthuis, S. G. E., and Hoffmann, A., "Giant magnetoresistance in ferromagnet/superconductor superlattices," *Phys. Rev. Lett.* **94**, 057002 (Feb 2005).

[13] Chakhalian, J., Freeland, J., Srajer, G., Strempfer, J., Khaliullin, G., Cezar, J., Charlton, T., Dalgliesh, R., Bernhard, C., Cristiani, G., et al., "Magnetism at the interface between ferromagnetic and superconducting oxides," *Nature Physics* **2**(4), 244–248 (2006).

[14] Aruta, C., Ghiringhelli, G., Dallera, C., Fracassi, F., Medaglia, P., Tebano, A., Brookes, N., Braicovich, L., and Balestrino, G., "Hole redistribution across interfaces in superconducting cuprate superlattices," *Physical Review B* **78**(20), 205120 (2008).

[15] Satapathy, D. K., Uribe-Laverde, M. A., Marozau, I., Malik, V. K., Das, S., Wagner, T., Marcelot, C., Stahn, J., Brück, S., Rühm, A., Macke, S., Tietze, T., Goering, E., Frañó, A., Kim, J. H., Wu, M., Benckiser, E., Keimer, B., Devishvili, A., Toperverg, B. P., Merz, M., Nagel, P., Schuppler, S., and Bernhard, C., "Magnetic Proximity Effect in $YBa_2Cu_3O_7/La_{2/3}Ca_{1/3}MnO_3$ and $YBa_2Cu_3O_7/LaMnO_{3+\delta}$ Superlattices," *Phys. Rev. Lett.* **108**, 197201 (May 2012).

[16] Tokura, Y., "Critical features of colossal magnetoresistive manganites," *Reports on Progress in Physics* **69**(3), 797 (2006).

[17] Keimer, B., Kivelson, S., Norman, M., Uchida, S., and Zaanen, J., "From quantum matter to high-temperature superconductivity in copper oxides," *Nature* **518**(7538), 179–186 (2015).

[18] Hwang, J., "Electron?boson spectral density function of correlated multiband systems obtained from optical data: $Ba_{0.6}K_{0.4}Fe_2As_2$ and LiFeAs," *Journal of Physics: Condensed Matter* **28**(12), 125702 (2016).

[19] Malik, V. K., Marozau, I., Das, S., Doggett, B., Satapathy, D. K., Uribe-Laverde, M. A., Biskup, N., Varela, M., Schneider, C. W., Marcelot, C., Stahn, J., and Bernhard, C., "Pulsed laser deposition growth of heteroepitaxial $YBa_2Cu_3O_7/La_{0.67}Ca_{0.33}MnO_3$ superlattices on $NdGaO_3$ and $Sr_{0.7}La_{0.3}Al_{0.65}Ta_{0.35}O_3$ substrates," *Phys. Rev. B* **85**, 054514 (Feb 2012).

[20] Matsumoto, N., Hosokura, T., Nagashima, T., and Hangyo, M., "Measurement of the dielectric constant of thin films by terahertz time-domain spectroscopic ellipsometry," *Optics letters* **36**(2), 265–267 (2011).

[21] Marsik, P., Sen, K., Khmaladze, J., Yazdi-Rizi, M., Mallett, B. P. P., and Bernhard, C., "Terahertz ellipsometry study of the soft mode behavior in ultrathin $SrTiO_3$ films," *Applied Physics Letters* **108**(5) (2016).

[22] Bernhard, C., Humlicek, J., and Keimer, B., "Far-infrared ellipsometry using a synchrotron light source the dielectric response of the cuprate high-t_c superconductors," *Thin Solid Films* **455**, 143–149 (2004).

[23] Hepting, M., Kukuruznyak, D., Benckiser, E., Tacon, M. L., and Keimer, B., "Raman light scattering on ultra-thin films of lanio3 under compressive strain," *Physica B: Condensed Matter* **460**(Supplement C), 196 – 198 (2015). Special Issue on Electronic Crystals (ECRYS-2014).

[24] Iliev, M. N., Abrashev, M. V., Lee, H.-G., Popov, V. N., Sun, Y. Y., Thomsen, C., Meng, R. L., and Chu, C. W., "Raman spectroscopy of orthorhombic perovskitelike $ymno_3$ and $lamno_3$," *Phys. Rev. B* **57**, 2872–2877 (Feb 1998).

[25] Dediu, V., Ferdeghini, C., Matacotta, F. C., Nozar, P., and Ruani, G., "Jahn-teller dynamics in charge-ordered manganites from raman spectroscopy," *Phys. Rev. Lett.* **84**, 4489–4492 (May 2000).

[26] Yamamoto, K., Kimura, T., Ishikawa, T., Katsufuji, T., and Tokura, Y., "Raman spectroscopy of the charge-orbital ordering in layered manganites," *Phys. Rev. B* **61**, 14706–14715 (Jun 2000).

[27] Martın-Carrón, L. and De Andrés, A., "Raman phonons and the Jahn-Teller transition in $RMnO_3$ manganites," *Journal of alloys and compounds* **323**, 417–421 (2001).

[28] Abrashev, M. V., Bäckström, J., Börjesson, L., Pissas, M., Kolev, N., and Iliev, M. N., "Raman spectroscopy of the charge- and orbital-ordered state in $la_{0.5}ca_{0.5}mno_3$," *Phys. Rev. B* **64**, 144429 (Sep 2001).

[29] Iliev, M. N., Abrashev, M. V., Popov, V. N., and Hadjiev, V. G., "Role of Jahn-Teller disorder in Raman scattering of mixed-valence manganites," *Phys. Rev. B* **67**, 212301 (Jun 2003).

[30] Tomioka, Y., Okimoto, Y., Jung, J. H., Kumai, R., and Tokura, Y., "Critical control of competition between metallic ferromagnetism and charge/orbital correlation in single crystals of perovskite manganites," *Phys. Rev. B* **68**, 094417 (Sep 2003).

[31] Driza, N., Blanco-Canosa, S., Bakr, M., Soltan, S., Khalid, M., Mustafa, L., Kawashima, K., Christiani, G., Habermeier, H.-U., Khaliullin, G., Ulrich, C., Le Tacon, M., and Keimer, B., "Long-range transfer of electron-phonon coupling in oxide superlattices," *Nature Materials* **11** (june 2012).

[32] Opel, M., Nemetschek, R., Hoffmann, C., Philipp, R., Müller, P., Hackl, R., Tüttő, I., Erb, A., Revaz, B., Walker, E., et al., "Carrier relaxation, pseudogap, and superconducting gap in high-T_c cuprates: A Raman scattering study," *Physical Review B* **61**(14), 9752 (2000).

[33] Limonov, M. F., Rykov, A. I., Tajima, S., and Yamanaka, A., "Superconductivity-induced effects on phononic and electronic raman scattering in twin-free $yba_2cu_3o_{7-x}$ single crystals," *Phys. Rev. B* **61**, 12412–12419 (May 2000).

[34] Bakr, M., Souliou, S. M., Blanco-Canosa, S., Zegkinoglou, I., Gretarsson, H., Strempfer, J., Loew, T., Lin, C. T., Liang, R., Bonn, D. A., Hardy, W. N., Keimer, B., and Le Tacon, M., "Lattice dynamical signature of charge density wave formation in underdoped $yba_2cu_3o_{6+x}$," *Phys. Rev. B* **88**, 214517 (Dec 2013).